PHILOSOPHICAL TRANSACTIONS OF THE ROYAL SOCIETY B BIOLOGICAL SCIENCES

The Aerodynamics of Hovering Insect Flight. II. Morphological Parameters

C. P. Ellington

Phil. Trans. R. Soc. Lond. B 1984 **305**, 17-40
doi: 10.1098/rstb.1984.0050

Phil. Trans. R. Soc. Lond. B **305**, 17–40 (1984)

Printed in Great Britain

THE AERODYNAMICS OF HOVERING INSECT FLIGHT. II. MORPHOLOGICAL PARAMETERS

By C. P. ELLINGTON

Department of Zoology, University of Cambridge, Downing Street, Cambridge CB2 3EJ, U.K.

(*Communicated by Sir James Lighthill, F.R.S.* – *Received* 28 *March* 1983)

CONTENTS

Morphological parameters are presented for a variety of insects that have been filmed in free flight. The nature of the parameters is such that they can be divided into two distinct groups: gross parameters and shape parameters. The gross parameters provide a very crude, first-order description of the morphology of a flying animal: its mass, body length, wing length, wing area and wing mass. Another gross parameter of the wings is their virtual mass, or added mass, which is the mass of air accelerated and decelerated together with the wing at either end of the wingbeat. The wing motion during these accelerations is almost perpendicular to the wing surface, and the virtual mass is approximately given by the mass of air contained in an imaginary cylinder

around the wing with the chord as its diameter. The virtual mass ranges from 0.3 to 1.3 times the actual wing mass, indicating that the total mass accelerated by the flight muscles can be more than twice the wing mass itself.

Over the limited size range of insects in this study, the interspecific variation of non-dimensional forms of the gross parameters is much greater than any systematic allometric variation, and no interspecific correlations can be found. The new shape parameters provide quite a surprise, however: intraspecific coefficients of variation are very low, often only 1%, and interspecific allometric relations are extremely strong.

Mechanical aspects of flight depend not only on the magnitude of gross morphological quantities, but also on their distributions. Non-dimensional radii are derived from the non-dimensional moments of the distributions; for example, the first radius of wing mass about the wing base gives the position of the centre of mass, and the second radius corresponds to the radius of gyration. The radii are called 'shape parameters' since they are functions only of the normalized shape of the distributions, and they provide a second-order description of the animal morphology. The various radii of wing area are strongly correlated, as are those of wing mass and of virtual mass: the higher radii for each quantity can all be expressed by allometric functions of the first radius. The overall shape of the distribution of a quantity can therefore be characterized by a single parameter, the position of the centroid of that quantity.

The strong relations between the radii of wing area, mass and virtual mass hold for a diverse collection of insects, birds and bats. Thus flying animals adhere to 'laws of shape' regardless of biological differences. Aerodynamic and mechanical considerations are most likely to provide an understanding of these laws of shape, but an explanation has proved elusive so far.

The detailed shape of a distribution can be reconstructed from the shape parameters by matching the moments of the observed distribution to those of a suitable analytical function. A Beta distribution is compared with the distribution of wing area, i.e. the shape of the wing, and a very good fit is found. With use of the laws of shape relating the higher radii to the first radius, the Beta distribution can be reduced to a function of only one parameter, thus providing a powerful tool for drawing a close approximation to the entire shape of a wing given only its centroid of area. Quite unexpectedly, the continuous spectrum of wing shapes can then be described in detail by a single parameter of shape.

1. Introduction

The morphological and kinematic variety of the insects makes them an ideal subject for a comparative analysis of hovering flight. Indeed, examples of the three groups of hovering animals discussed in paper I are readily collected from most gardens, and this study is based on such 'common or garden' species. The Diptera and Hymenoptera are especially proficient at hovering and, therefore, receive the greatest attention. Although the Odonata provide a superb example of hovering with an inclined stroke plane, they are being investigated elsewhere (D. Newman, personal communication) and have been omitted here.

Accurate morphological data are a necessary foundation for any aerodynamic study, and the data presented here are primarily intended for use in the mechanical analyses of paper VI. Morphological parameters were measured immediately after the insects had been filmed in free flight; the filming is described in paper III. A few parameters could not be determined on the fresh insects because of time limitations, and so were taken from other specimens of the same species. For comparative purposes the parameters are generally reduced to non-dimensional forms, which prove remarkably constant for each species.

PHILOSOPHICAL TRANSACTIONS OF THE ROYAL SOCIETY B BIOLOGICAL SCIENCES

Weis-Fogh (1973) separated the quasi-steady aerodynamic integrals for hovering flight into morphological and kinematic parameters, showing that the aerodynamic force and profile power are proportional to the second and third moments of the wing area, respectively. His approach is extended in this paper, and a new set of parameters characterizing the wing shape and mass distribution is derived from the moments of area, mass and virtual mass of the wings. In paper VI many integral expressions of physical quantities can then be reduced to forms proportional to the moment parameters.

2. Materials and methods

The choice of insects was usually quite arbitrary within the framework of selecting ones proficient at slow or hovering flight in the field. As will be seen in paper III, however, this did not guarantee a good flight performance under laboratory conditions. The seven-spot ladybird *Coccinella 7-punctata* (Coccinellidae) is readily available and was chosen as a token coleopteran, which are generally slow steady fliers without much manoeuvring capability. Dipteran flight seems more interesting and varied, and the selection here is somewhat more deliberate: crane-flies *Tipula obsoleta* and *T. paludosa* (Tipulidae), representing the primitive suborder Nematocera; the hover-fly *Episyrphus balteatus* (Syrphidae, Syrphinae); and the drone-fly *Eristalis tenax* (Syrphidae, Milesiinae). The last two insects belong to the large family Syrphidae, which are collectively called 'hover-flies'. Wing venation is reduced in this family, as with all of the more advanced Diptera, and the wing has a 'false margin' of cross veins along the trailing edge. Members of the subfamily Syrphinae usually hover with an inclined stroke plane, and Weis-Fogh (1973) called these the 'true' hover-flies. Flies of the other subfamily Milesiinae tend to be bulkier, with higher wing loadings, and, to judge from *Eristalis* and *Volucella*, prefer to hover with a horizontal stroke plane although they are often seen using an inclined one. Even if this functional difference between the subfamilies is more generally valid, it is hardly fair to label the Syrphinae as 'true' hover-flies, implying that the Milesiinae are 'false' – they are equally superb fliers.

The Hymenoptera must be represented in any study of hovering flight, and common species of the large superfamily Apoidea have been included: the honey bee *Apis mellifera*, various species of the bumble bee *Bombus*, and the cuckoo bee *Psithyrus vestalis*, which parasitizes bumble bees and is very similar to them in morphology. Within the Lepidoptera, many of the moths are proficient slow fliers. Weis-Fogh (1973) had already filmed the large hawk moth *Manduca sexta* (Sphingidae), and so two small moths were chosen for contrast. One of these, the common plume moth *Emmelina monodactylus* (Pterophoridae), also complemented R. Å. Norberg's (1972*a*) multiple-exposure photographic study of two other plume moths. The other example was *Ephestia kuehniella*, a member of the large family of small moths Pyralidae. The filming of this insect was unsuccessful, as described in paper III, so morphological data were not taken. Finally a specimen was chosen from the Neuroptera, an ancient order with uncoupled flimsy wings with a delicate network of veins. The green lacewing *Chrysopa carnea* (Chrysopidae) is the best known British member of the order, and is generally considered to be a 'weak' flier. Another neuropteran had been filmed previously by Weis-Fogh (unpublished): *Pterocroce capillaris* of the family Nemopteridae, which are recognized by long ribbon-like hindwings that trail behind passively in flight.

The insects were collected locally in the mornings, and used in experiments upon return to

PHILOSOPHICAL TRANSACTIONS OF THE ROYAL SOCIETY B BIOLOGICAL SCIENCES

the laboratory. They were anaesthetized with CO_2 after filming, and the total mass m was measured to an accuracy of ± 0.1 mg on an electrobalance. Specimens were identified later by Mr D. M. Unwin. The high-speed films and morphological notes of Weis-Fogh were available to me, and his data for *Manduca* and *Pterocroce* (collected in the Atlas Mountains of Morocco by Mr R. Northfield) were considered in this study. The morphological parameters presented in this paper for *Manduca* were measured from specimens reared in the Departmental Field Station on a semi-synthetic diet (Hoffman *et al.* 1966).

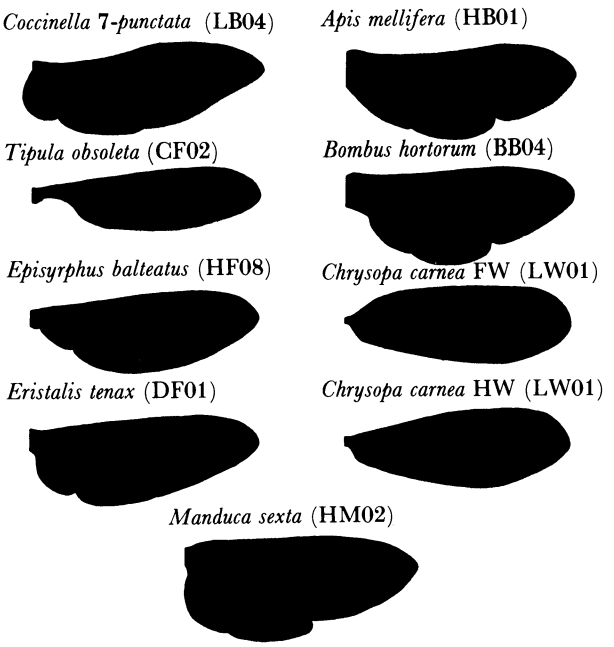

FIGURE 1. Planforms, or wing outlines, of some of the insects used in this study. Only the hindwing is shown for *Coccinella*; the forewing (FW) and hindwing (HW) are given separately for *Chrysopa*, and are coupled together for *Apis*, *Bombus* and *Manduca*. Identification codes for the insects are enclosed in parentheses and explained in the text.

2.1. *Wing planform*

The planform, or outline, of the wing proves to be a dominant factor in the aerodynamic analysis of hovering flight (paper VI), and examples are shown in figure 1. Detailed measurements of the planform were made as follows. Immediately after weighing the insects, the right wing, or wing pair, was cut from the body and weighed to ± 1 μg; the other wing was left attached to aid identification. The severed wing was placed between two glass slides and mounted in an enlarger. With use of the wing as a negative, prints were made at about $\times 13$ magnification. A grid negative was also printed to determine magnification and to check distortions in the photographic process, which always proved negligible. The basal hinge line was drawn on each print, and the wing base was arbitrarily defined as the point on that line one-third of the distance from the leading edge to the trailing edge (figure 2*a*). The line connecting the wing base and the wing tip is called the longitudinal wing axis. The wing length R was measured between these two points to an accuracy of better than $\pm 0.5\%$: the error was primarily due to difficulty in defining the hinge line on the prints.

Coordinates of the wing outline were then determined at intervals of 0.02 R on the prints by using the digitizer described in paper III. Fifty values of the chord c, the distance between the leading and trailing edges, were thus obtained along the wing length. The small but dense fringe of hairs around the neuropteran wings (*Pterocroce* and *Chrysopa*) should slightly increase the aerodynamically effective wing area: the leading and trailing edges were arbitrarily taken along the middle of the fringes for these wings. Prints of the forewing and hindwing of *Manduca* were overlapped to provide a wing outline corresponding to that observed during flight.

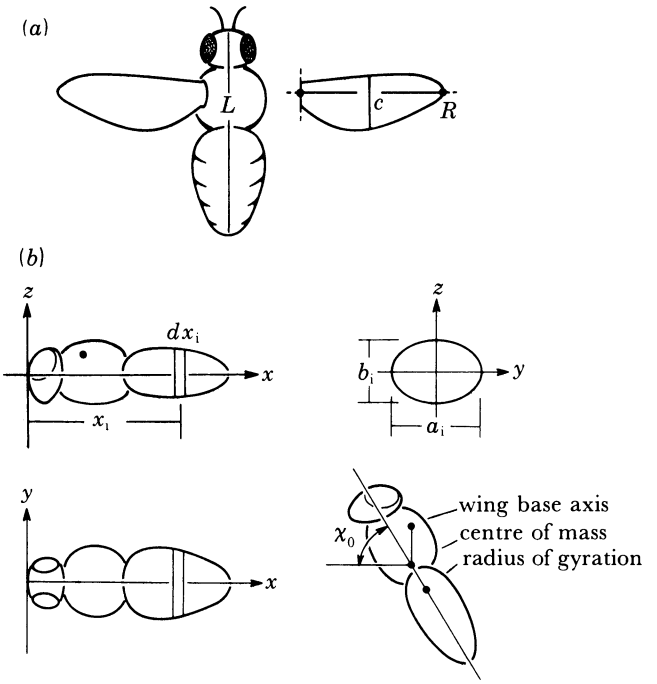

FIGURE 2. (*a*) Definitions of body length L, wing length R, and chord c, are illustrated. The longitudinal wing axis and hinge line are drawn for the severed wing. (*b*) The coordinate system and parameters used in the graphical method of estimating the mass distribution of the body. Locations of the centre of mass and radius of gyration are shown, as well as the definition of the free body angle χ_0.

It was necessary to take wing measurements of *Emmelina* in a different manner, because the plumes could not be arranged accurately for the severed wing. The wing length was found directly by using a measuring magnifier, and a print of the wing shape was made from a cine film frame that showed the wing area maximally projected during flight. The plume fringes are very dense, so the wing outline was taken along perimeter of the fringe areas.

2.2. *Wing mass distribution*

The moment of inertia I of a wing about its base depends on the distribution of mass along the wing, and it must be known in order to calculate the inertial torque and power during flapping flight. It was not possible to determine I for the filmed insects in addition to the other procedures, and so values were either taken from the study of Sotavalta (1952) or measured from fresh specimens by the normal strip-weighing technique. A wing was cut from the insect and weighed, and R was determined directly with the magnifier. The wing was then placed

on 1 mm graph paper and, beginning at the wing base, 2 mm wide strips were sequentially cut perpendicular to the wing axis and weighed to ± 0.5 μg. This procedure was done as quickly as possible to minimize mass loss through evaporation. The distance r_i from the wing base to the centre of mass for each strip was taken as that to the geometrical centre of a strip. The moment of inertia of the wing was calculated as

$$I = \Sigma\, m_i\, r_i^2, \tag{1}$$

where m_i is the mass of a particular strip.

The sum of the masses of the strips, $\Sigma\, m_i$, was typically 5–10 % less than the initial wing mass. For some specimens of *Episyrphus* and *Chrysopa* the remainder of the wing was also weighed after each strip, which revealed that a roughly constant mass was lost with each cut. The mass of each strip was then corrected in equation (1) to provide a better estimate of I. This value differed by only 2 % from that of a much simpler correction, however: the original values of m_i were used in equation (1), and the moment of inertia was multiplied by the ratio of initial wing mass to $\Sigma\, m_i$. This latter correction is sufficiently accurate, and has been applied to all values of I determined by strip-weighing.

The moment of inertia for *Manduca* wings was found by a compound pendulum technique, which proved much easier than the other method and virtually eliminated problems of mass loss. A forewing was cut from an anaesthetized insect, and its mass and length were measured. A fine entomological pin was then stuck through the wing base such that the plane of the wing was perpendicular to the pin. The pin was rested on two parallel horizontal rods; on one of the rods a fine thread weighted at one end provided a vertical reference. The wing was photographed in this position, and then gently tapped so that it oscillated as a pendulum and cyclically interrupted a light beam falling on a photodiode. The period of oscillation T was measured over about 20 cycles using a storage oscilloscope connected to the photodiode signal. The pin was then stuck through the wing near the trailing edge at about $\frac{1}{3}R$, replaced on the two rods, and a photograph was taken again. The centre of mass for the wing was easily located from the photographs, and the distance from it to the wing base was measured. The procedure was then repeated on the hindwing.

The moment of inertia for any undamped compound pendulum oscillating about a given axis can be derived as

$$I = rmgT^2/4\pi^2, \tag{2}$$

where m is the mass, r is the distance from that axis to the centre of mass, g is gravitational acceleration and T is the period. This procedure may be used to determine I for any arbitrary body when damping is small and when the pin makes a negligible contribution to the total moment of inertia. It proved very satisfactory for *Manduca* wings, but for smaller insects the damping was too large.

2.3. *Body morphology*

The length and mass distribution of the insect bodies were determined and used to derive morphological parameters for the body. The manner in which some flight characteristics depend on body morphology is discussed in §4.2.1., and the parameter estimates need not be very accurate for this purpose. A graphical method based on the flight films was used to determine the mass distribution of the body for all insects except *Manduca*.

For each insect, two cine frames were selected that showed lateral and dorsoventral views

of the body. The body length L was measured as a proportion $\hat{L}$ of the wing length in the film sequence. Prints were made of these two frames at about $\times 13$ magnification. A longitudinal body axis was drawn on the lateral view, approximately cutting the body into dorsal and ventral halves. The body was divided into n strips (typically 20) perpendicular to this axis, and corresponding divisions were drawn on the other view. Figure 2*b* shows the procedure and the coordinate system employed. The body outline was chosen to include the coxa, but the more distal leg segments and the wings were ignored because their mass contribution could not be treated by this technique. The neglected mass is relatively small, however, and should not significantly affect the parameters. A uniform mass density was assumed for the body, and the cross-section was taken as elliptical. The characteristics of each section i of the body are its thickness $\mathrm{d}x_\mathrm{i}$, distance from the anterior end x_i, and widths a_i and b_i; all dimensions are expressed as a fraction of the body length on the appropriate print. The mass of each elliptical section is proportional to its volume, $\frac{1}{4}\pi a_\mathrm{i} b_\mathrm{i} \mathrm{d}x_\mathrm{i}$.

The position of the forewing base axis was located on the lateral view. The moment of inertia of the body I_b was taken about this axis, and thus applies to pitching movements of the insect. The body parameters of interest and their calculation from the estimated mass distribution are derived in §3.2.

The compound pendulum technique was used to determine these parameters for *Manduca* specimens. They were heavily anaesthetized for the procedure, and the wings were removed. The pin was located first through the wing bases, and then through the third abdominal segment near the dorsal surface.

3. Definitions and results

Non-dimensional forms of parameters, denoted by a circumflex accent, or 'hat', are used extensively in this comparative study. It is thus necessary to present only two gross morphological measurements in absolute units: the total mass m, and the wing length R.

Table 1 lists the insects studied and their values of the morphological parameters. An identification code ID is assigned to each specimen for later reference. The forewings and hindwings of the lacewing *Chrysopa* beat out of phase during flight, and so are treated separately in the table. The elytra of the ladybird *Coccinella* do not contribute significantly to the aerodynamics of hovering, and wing parameters are given for the membranous hindwings only. For the remaining insects either the forewings and hindwings are coupled together or the hindwings are not effective aerodynamically: the wing parameters then refer to the single functional pair of wings.

The wing mass m_w includes right and left wings, and is expressed as a fraction $\hat{m}_\mathrm{w}$ of the total mass. The wing loading equals the weight mg divided by the total sustaining wing area. This is the mean pressure exerted on the air by the wings during hovering and, therefore, is denoted by p_w.

Weis-Fogh's notes on the nemopterid *Pterocroce* were incomplete, and its mass has been estimated from the other neuropteran, *Chrysopa*. Fortunately the body shapes are similar (§4.2.1. and table 2), and so the mass was estimated by using the mean value of m divided by the cube of the body length from five specimens of *Chrysopa*. The wing loading of *Pterocroce* relies on this mass estimate, and both values are enclosed in square brackets in table 1.

PHILOSOPHICAL TRANSACTIONS OF THE ROYAL SOCIETY B BIOLOGICAL SCIENCES

PHILOSOPHICAL TRANSACTIONS OF THE ROYAL SOCIETY B BIOLOGICAL SCIENCES

TABLE 1. TOTAL MASS AND MORPHOLOGICAL WING PARAMETERS

(All insects execpt *Manduca* and *Aeschna* were filmed in free flight immediately before measurements were taken. Estimated values of parameters are enclosed in square brackets and are explained in the text. Coefficients of variation for the mean values of the wing mass radii are given in parentheses below each value; original sources for the data are indicated by the reference number, with the number of samples enclosed in parentheses. Parameters for some of the animals discussed in paper I are also presented, and are calculated from data in the references. References are numbered as follows: 1, Sotavalta (1952); 2, present study; 3, R. Å. Norberg (1972*b*); 4, Weis-Fogh (1972); 5, U. M. Norberg (1975); 6, U. M. Norberg (1976). FW, forewing; HW, hindwing; w after the sex of *Apis mellifera* stands for 'worker'.)

species	sex	ID	m mg	R mm	p_w N m^{-2}	$\mathcal{R}$	$r_1(S)$	$r_2(S)$	$r_3(S)$	$\hat{v}$	$r_1(v)$	$r_2(v)$	$\int \hat{c}^2 r^2 dr$	$\int \hat{c}^{\frac{3}{2}} r^{\frac{5}{2}} dr$	m_w(%)	$\hat{h}$(%)	$r_1(m)$	$r_2(m)$	ref.
Coleoptera																			
Coccinella 7-punctata	F	LB01	35.9	11.7	4.61	7.17	0.463	0.528	0.575	1.07	0.448	0.504	0.526	0.218	2.67	0.0894			
	F	LB02	26.7	11.0	3.85	7.11	0.467	0.533	0.580	1.07	0.457	0.514	0.531	0.226	2.82	0.0838			
	M	LB03	23.7	10.3	3.84	7.01	0.467	0.533	0.580	1.07	0.456	0.513	0.531	0.225	2.92	0.0925	[0.32]	[0.40]	1
	F	LB04	34.4	11.2	4.76	7.07	0.463	0.528	0.574	1.08	0.452	0.507	0.542	0.220	2.87	0.1035			
	M	LB05	30.7	10.8	4.57	7.08	0.463	0.529	0.575	1.07	0.451	0.507	0.534	0.220	2.55	0.0917			
Diptera																			
Tipula obsoleta	M	CF01	19.0	13.7	2.59	10.45	0.555	0.603	0.639	1.16	0.576	0.611	0.835	0.329	[3.38]	[0.0544]			
	M	CF02	11.4	12.7	1.89	10.93	0.555	0.602	0.638	1.17	0.574	0.608	0.841	0.328	[4.29]	[0.0544]	[0.41]	[0.50]	2
T. paludosa	M	CF03	34.6	16.2	3.75	11.59	0.554	0.601	0.637	1.17	0.577	0.610	0.857	0.328	2.94	0.0578			
	M	CF04	49.8	17.4	4.54	11.25	0.556	0.604	0.640	1.17	0.580	0.614	0.857	0.332	2.37	0.0525	0.41 (1.5%)	0.50 (2.2%)	2 ($n = 3$)
	M	CF05	43.1	17.2	3.94	11.04	0.547	0.595	0.631	1.17	0.565	0.599	0.827	0.316	2.71	0.0528			
Episyrphus balteatus	M	HF01	51.5	10.2	10.60	8.73	0.506	0.561	0.602	1.11	0.512	0.554	0.671	0.264	0.89	0.0786			
	M	HF02	42.1	10.0	8.53	8.26	0.508	0.563	0.604	1.11	0.514	0.556	0.672	0.266	0.84	0.0609			
	M	HF03	34.7	10.2	6.65	8.13	0.500	0.558	0.600	1.10	0.505	0.549	0.640	0.258	0.93	0.0515			
	M	HF04	29.3	9.7	6.40	8.38	0.505	0.562	0.603	1.10	0.511	0.555	0.653	0.264	1.45	0.0813			
	M	HF05	41.2	9.9	8.72	8.46	0.502	0.559	0.601	1.10	0.507	0.551	0.646	0.260	1.34	0.1003	0.36 (6.6%)	0.44 (5.3%)	2 ($n = 6$)
	F	HF06	14.0	9.0	3.52	8.31	0.516	0.570	0.609	1.12	0.525	0.565	0.699	0.276	1.89	0.0628			
	M	HF07	27.3	9.3	6.54	8.45	0.510	0.565	0.606	1.11	0.517	0.560	0.670	0.270	1.27	0.0759			
	F	HF08	28.1	10.0	5.46	7.92	0.511	0.565	0.605	1.12	0.519	0.559	0.690	0.269	1.49	0.0691			
	M	HF09	14.2	7.7	4.90	8.35	0.514	0.568	0.609	1.11	0.522	0.563	0.684	0.273	1.48	0.0801			
	M	HF10	22.2	9.5	4.98	8.25	0.507	0.562	0.603	1.11	0.512	0.554	0.666	0.265	1.68	0.0748			
	M	HF11	25.4	9.5	5.80	8.41	0.509	0.564	0.605	1.11	0.517	0.559	0.672	0.268	1.44	0.0747			
Eristalis tenax	F	DF01	68.4	11.4	9.23	7.15	0.471	0.534	0.579	1.09	0.457	0.509	0.549	0.225	[1.54]	[0.106]	[0.32]	0.4 (7.4%)	1 ($n = 7$)
	M	DF02	112.0	11.1	16.5	7.39	0.481	0.542	0.586	1.09	0.474	0.523	0.578	0.236	0.84	0.106			
Hymenoptera																			
Apis mellifera	F_w	HB01	101.9	9.8	17.5	6.74	0.480	0.544	0.589	1.07	0.476	0.529	0.561	0.239	0.50	0.0760			
	F_w	HB02	97.2	9.5	17.6	6.65	0.480	0.543	0.589	1.07	0.474	0.527	0.557	0.237	0.56	0.0880			
	F_w	HB03	87.3	9.3	16.6	6.71	0.484	0.545	0.589	1.09	0.481	0.529	0.593	0.240	0.43	0.0652	[0.37]	0.45 (3.5%)	1 ($n = 4$)
	F_w	HB04	97.1	9.6	17.0	6.58	0.482	0.545	0.590	1.07	0.478	0.529	0.566	0.240	0.35	0.0527			
	F_w	HB05	87.2	9.4	15.9	6.59	0.478	0.541	0.587	1.07	0.471	0.524	0.556	0.235	0.47	0.0677			
Psithyrus vestalis	M	BB01	188	14.3	14.6	6.47	0.490	0.549	0.592	1.10	0.486	0.531	0.610	0.244	0.69	0.0598			
	M	BB02	157	13.8	13.5	6.68	0.480	0.538	0.581	1.11	0.473	0.517	0.614	0.231	0.74	0.0615			
Bombus terrestris	M	BB03	223	14.3	17.1	6.40	0.482	0.542	0.587	1.09	0.473	0.521	0.584	0.235	0.68	0.0691			
B. hortorum	M	BB04	226	14.1	18.8	6.73	0.482	0.541	0.584	1.10	0.475	0.521	0.603	0.234	0.48	0.0543			
B. agrorum	M	BB05	174	11.4	21.3	6.49	0.499	0.557	0.600	1.09	0.501	0.547	0.623	0.257	0.47	0.0746	[0.36]	0.44 (2.9%)	1 ($n = 3$)
B. terrestris	M	BB06	266	14.2	22.6	6.98	0.486	0.545	0.588	1.10	0.483	0.529	0.612	0.240	0.50	0.0675			
B. agrorum	M	BB07	143	11.4	18.3	6.79	0.501	0.558	0.600	1.10	0.504	0.548	0.641	0.258	0.53	0.0724			
B. lucorum	M	BB08	231	14.1	19.5	6.83	0.483	0.543	0.587	1.10	0.475	0.522	0.593	0.236	0.59	0.0692			
Lepidoptera																			
Emmelina monodactylus	F	PM01	8.4	11.1	0.97	5.79	0.446	0.510	0.556	1.11	0.427	0.482	0.533	0.200	—	—	—	—	
Manduca sexta	M	HM01	1320	51.8	6.60	5.47	0.430	0.499	0.549	1.10	0.393	0.453	0.468	0.184	6.02	0.0652			
	F	HM02	1584	48.7	9.50	5.80	0.440	0.508	0.558	1.09	0.409	0.469	0.479	0.194	4.85	0.0804	0.32 (1.9%)	0.43 (2.9%)	2 ($n = 3$)
	M	HM03	1388	46.0	8.96	5.57	0.438	0.507	0.557	1.09	0.404	0.464	0.470	0.191	4.62	0.0764			
	F	HM04	1344	51.8	7.17	5.84	0.436	0.504	0.553	1.10	0.403	0.461	0.485	0.188	—	—			
Neuroptera																			
Pterocroce capillaris	M	NE01	[3.8]	10.0	[0.95]	10.23	0.563	0.610	0.645	1.17	0.592	0.625	0.883	0.343	[3.42]	[0.0279]	—	—	
Chrysopa carnea (FW)	F	LW01	11.2	14.0	0.59	7.53	0.529	0.584	0.625	1.10	0.545	0.589	0.699	0.298	4.50	0.0288	0.44 (5.1%)	0.52 (3.4%)	2 ($n = 5$)
(HW)	—	—	—	12.7		7.93	0.534	0.587	0.625	1.12	0.556	0.595	0.752	0.304	3.05	0.0276			
(FW)	F	LW02	9.0	13.4	0.57	8.19	0.533	0.587	0.627	1.10	0.552	0.595	0.719	0.304	4.55	0.0290	0.47 (2.6%)	0.55 (2.1%)	
(HW)	—	—	—	12.0		8.46	0.542	0.594	0.632	1.12	0.569	0.607	0.781	0.316	2.89	0.0265			
Odonata																			
Aeschna juncea (FW)	—	—	754	47.4	4.15	11.63	0.507	0.567	0.610	1.07	0.516	0.565	0.619	0.272	1.07	0.0184	0.45	0.53	3
(HW)	—	—	—	46.0		8.40	0.446	0.518	0.569	1.06	0.414	0.481	0.451	0.205	1.12	0.0152	0.38	0.47	
Birds																			
Amazilia fimbriata fluviatilis	—	—	5100	58.5	28.5	7.80	0.420	0.487	0.538	1.14	0.378	0.433	0.485	0.171	6.06	0.2509	0.26	0.33	4
Ficedula hypoleuca	—	—	12000	100	13.0	4.41	0.427	0.503	0.557	1.08	0.378	0.450	0.413	0.186	[11]	[0.1213]	—	—	5
Bats																			
Plecotus auritus	—	—	9000	124	8.71	6.07	0.420	0.494	0.546	1.10	0.374	0.445	0.432	0.179	12.9	0.0770	0.26	0.35	6

3.1. *Moment parameters of the wings*

Most of the remaining parameters in table 1 are aptly described as moment parameters. The basic quantities of area, mass and virtual mass may be considered as variables defined over the wing length.The moments of these quantities about the wing base may then be used as parameters of the variable distribution along the wing, which is analogous to the characterization of distribution functions in probability theory by the moments of the distribution. As in that application, functions of these parameters are often of more interest than the distribution itself.

3.1.1. *Wing area*

Consider first the strip of wing area dS located at a distance r form the wing base and equal to $c\,\mathrm{d}r$. The total area S of the wing pair is given by

$$S = 2\int_0^R c\,\mathrm{d}r, \tag{3}$$

but may be expressed more conveniently by the non-dimensional aspect ratio $\mathcal{AR}$:

$$\mathcal{AR} = 4R^2/S. \tag{4}$$

The mean chord $\bar{c}$ of the wings is equal to the area divided by the span, $S/2R$, and is used to define a normalized chord $\hat{c}$ as

$$\hat{c} = c/\bar{c} = 2Rc/S = \tfrac{1}{2}\mathcal{AR}c/R. \tag{5}$$

It will also prove useful to introduce a non-dimensional radius $\hat{r}$ equal to r/R.

The kth moment of wing area S_k is defined by

$$S_k = 2\int_0^R c\,r^k\,\mathrm{d}r = SR^k\int_0^1 \hat{c}\,\hat{r}^k\,\mathrm{d}\hat{r}. \tag{6}$$

For a given wing length and area, the moments of area depend only on the distribution of the normalized chord along the wing: the *shape* of the wing. The aspect ratio may then be interpreted as a *scaling factor* for the wing shape. Non-dimensional moments are obtained by dividing S_k by SR^k, and the kth root may be taken to derive a non-dimensional radius of the kth moment of wing area:

$$\hat{r}_k^k(S) = S_k/SR^k = \int_0^1 \hat{c}\,\hat{r}^k\,\mathrm{d}\hat{r}. \tag{7}$$

That is, if all the wing area were located at a distance $\hat{r}_k(S)$ from the wing base, the kth moment of area would then equal S_k. The values of $\hat{r}_k(S)$ are characteristic of the wing shape, and may be used to calculate S_k directly.

Weis-Fogh (1973) showed that the mean lift force in the quasi-steady analysis is proportional to the second moment of wing area, and that the mean profile power is proportional to the third moment. Values of $\hat{r}_k(S)$ are therefore presented in table 1 for k equal to 1, 2 and 3, together with the aspect ratio. This set of parameters is preferred to the shape factors of Weis-Fogh (1973) because a similar set proves useful for the mass and virtual mass of the wings.

PHILOSOPHICAL TRANSACTIONS OF THE ROYAL SOCIETY B BIOLOGICAL SCIENCES

3.1.2. *Wing mass*

The mass per unit length of the wing m' is used to define a similar moment set,

$$m_k = 2\int_0^R m' r^k \, \mathrm{d}r = m_w R^k \int_0^1 \hat{m}' \hat{r}^k \, \mathrm{d}\hat{r}, \tag{8}$$

where the normalized mass per unit length $\hat{m}'$ equals $2m'R/m_w$. The wing mass m_w is equal to m_k when k is zero. The radius for the kth moment of wing mass is given by

$$\hat{r}_k^k(m) = m_k/m_w R^k = \int_0^1 \hat{m}' \hat{r}^k \, \mathrm{d}\hat{r}, \tag{9}$$

and again depends only on the normalized distribution of the variable considered.

The first moment of mass is proportional to the resultant inertial force acting on the wings in flapping flight. The resultant force on each wing acts through its centre of mass, which is located at $\hat{r}_1(m)$. The second moment of mass is the moment of inertia of the wing pair I_w, equal to twice the value of I in equation (1), and is proportional to the inertial torque of the flapping wings. The radius of gyration of I_w is equal to $\hat{r}_2(m)$, and may be calculated from published data as

$$\hat{r}_2(m) = (I_w/m_w R^2)^{\frac{1}{2}}. \tag{10}$$

The compound pendulum technique is especially convenient for determining these parameters since $\hat{r}_1(m)$ is found directly, and $\hat{r}_2(m)$ is readily calculated from equations (2) and (10).

Table 1 presents mean values of $\hat{r}_1(m)$ and $\hat{r}_2(m)$ determined from other specimens of each species, since time limitations prevented measurement of the wing mass distribution for insects that were filmed. The original source of data is indicated by the reference, with the number of samples enclosed in parentheses. Coefficients of variation, equal to the sample standard deviation expressed as a percentage of the mean, are given in parentheses below $\hat{r}_1(m)$ and $\hat{r}_2(m)$; these coefficients have been adjusted for small sample size according to Sokal & Braumann (1980). When data from Sotavalta (1952) were used, $\hat{r}_1(m)$ was estimated from $\hat{r}_2(m)$ by using equation (26) of §4.2.2(*a*). Estimated values are indicated by square brackets: the radii of wing mass for *Tipula obsoleta* are taken from means of *T. paludosa*; a value of 0.40 for $\hat{r}_2(m)$ is assumed for *Coccinella*, based on values of 0.41 for the cockchafer *Melolontha vulgaris* and 0.39 for a longhorn beetle *Cerambycidae* (Sotavalta 1952).

Although it is very convenient, the non-dimensional wing mass $\hat{m}_w$ is not a very 'clean' parameter. The absolute wing mass is proportional to the product of wing area and the mean wing thickness, and is thus affected by variations in two parameters already used, R and $\mathcal{AR}$. When m_w is divided by the mass m, which has a large variance, the resulting parameter is sensitive to too many factors. A more independent measure of the wing mass would be the mean wing thickness, expressed as a fraction $\hat{h}$ of the wing length and defined by

$$\hat{h} = \frac{m_w}{\rho_w S R} = \frac{m_w \mathcal{AR}}{4\rho_w R^3}, \tag{11}$$

where the mass density of the wing ρ_w can be assigned the value for solid cuticle, 1200 kg m^{-3} (Jensen & Weis-Fogh 1962; Wainwright *et al.* 1976). Values of $\hat{h}$ are given in table 1. Estimated values were necessary for *Tipula obsoleta*, *Eristalis* (DF01), and *Pterocroce*; they were taken from *Tipula paludosa*, *Eristalis* (DF02) and *Chrysopa*, respectively, and were also used to estimate $\hat{m}_w$.

3.1.3. *Wing virtual mass*

Osborne (1951) suggested that acceleration forces could play a significant role in the aerodynamics of flapping flight. When a wing, or any body immersed in a fluid, is accelerated, it must set the surrounding air in motion. The inertia of the wing is increased by the mass of air that is accelerated, and so there is an apparent increase in the wing mass: the *virtual mass*, or added mass. Inviscid flow theory shows that the virtual mass of a thin wing accelerated normal to its chord is equal to the mass of air in an imaginary circular cylinder around the wing with the chord as its diameter. A wing section thus has a virtual mass v' per unit span equal to

$$v' = \tfrac{1}{4}\rho\pi c^2, \tag{12}$$

where ρ is the mass density of air. The total virtual mass of the wing pair is given by

$$v = 2\int_0^R v'\,\mathrm{d}r = \tfrac{1}{2}\rho\pi\bar{c}^2 R\int_0^1 \hat{c}^2\,\mathrm{d}\hat{r} = \frac{2\rho\pi R^3}{A R^2}\int_0^1 \hat{c}^2\,\mathrm{d}\hat{r}. \tag{13}$$

The proportionality constants in the expanded forms are equal to the virtual mass of a wing pair with span $2R$ and chord $\bar{c}$, the mean chord. Dividing v by this quantity, we derive an appropriate non-dimensional form

$$\hat{v} = \frac{v A R^2}{2\rho\pi R^3} = \int_0^1 \hat{c}^2\,\mathrm{d}\hat{r}. \tag{14}$$

The moments of virtual mass are defined by

$$v_k = 2\int_0^R v' r^k\,\mathrm{d}r = \frac{v R^k}{\hat{v}}\int_0^1 \hat{c}^2\hat{r}^k\,\mathrm{d}\hat{r}, \tag{15}$$

and the corresponding radii are

$$\hat{r}_k^k(v) = \frac{v_k}{v R^k} = \frac{1}{\hat{v}}\int_0^1 \hat{c}^2\hat{r}^k\,\mathrm{d}\hat{r}. \tag{16}$$

Values of $\hat{v}$, $\hat{r}_1(v)$ and $\hat{r}_2(v)$ are presented in table 1; the mechanical interpretations of the moments and radii of virtual mass are the same as for the wing mass itself.

Values of two more integrals will be required for the aerodynamic analysis in paper VI, and are given in table 1. They are moment parameters of the wing shape as well, but a direct physical interpretation cannot be assigned to them.

Some of the hovering animals discussed in paper I are also included in table 1 for comparison. The moment parameters for wing area and virtual mass were calculated from drawings of the wing outline in the references. The wing mass distribution, if given, was used to calculate $\hat{r}_1(m)$ and $\hat{r}_2(m)$. The wing mass for *Ficedula* is taken from Magnan (1922).

3.2. *Body parameters*

The lateral and dorsoventral views of the body required for the graphical technique could not be obtained for some filmed insects. Mean values of the derived body parameters are therefore presented in table 2, together with the coefficients of variation and the number of samples n.

The body length L is expressed as a fraction $\hat{L}$ of the wing length. All other body parameters with linear dimensions are given as a fraction of the body length.

Some mechanical analyses of flight require an estimate of the aerodynamic forces on the body.

However, the flow conditions near the body cannot be described accurately because of the complexity of the induced velocity field. The aerodynamic force estimate will be a crude approximation at best, and it will be sufficient to consider the body as a circular cylinder of length L. By equating the mass of the cylinder with that of the insect, a mean diameter $\hat{d}$ as a fraction of body length can be calculated by

$$\hat{d} = (4m/\pi\bar{\rho}_b L^3)^{\frac{1}{2}}, \tag{17}$$

where $\bar{\rho}_b$ is the mean mass density of the body. The mean body density should lie between 1200 kg m^{-3} for solid cuticle and a value closer to 1000 kg m^{-3} for soft tissues. A mean density

TABLE 2. MEAN VALUES OF THE BODY PARAMETERS FOR INSECTS IN THIS STUDY

(The number of samples n is presented, and the coefficient of variation expressed as a percentage is given in parentheses after each mean value. Estimated values are enclosed in square brackets.)

species	n	$\hat{L}$	$\hat{d}$	$\hat{l}$	$\hat{l}_1$	$\hat{l}_2$	$\frac{\chi_0}{\text{deg}}$
Coleoptera							
Coccinella	5	0.73 (6.7)	0.26 (9.6)	—	—	—	—
Diptera							
Tipula obsoleta	2	0.85 (2.6)	0.11 (14.6)	0.45 (1.8)	0.21 (0)	0.34 (2.4)	70 (6.9)
T. paludosa	3	1.04 (1.9)	0.10 (1.3)	0.44 (3.8)	0.23 (4.6)	0.37 (3.4)	70 (1.8)
Episyrphus	4	1.10 (4.4)	0.16 (11.7)	0.41 (4.8)	0.14 (14)	0.29 (4.4)	53 (14)
Eristalis	2	1.22 (4.4)	0.20 (17)	0.48 (1.7)	0.12 (0)	0.26 (0)	50 (3.2)
Hymenoptera							
Apis	4	1.62 (4.9)	0.17 (7.0)	0.46 (1.4)	0.26 (9.1)	0.36 (3.8)	53 (2.9)
Psithyrus and *Bombus*	4	1.47 (3.3)	0.18 (16)	0.47 (3.7)	0.24 (16)	0.37 (9.4)	52 (3.8)
Lepidoptera							
Emmelina	1	0.78	0.12	0.41	0.25	0.36	76
Manduca	3	0.81 (3.8)	0.16 (9.5)	0.51 (2.5)	0.27 (12)	0.38 (7.3)	73 (3.1)
Neuroptera							
Pterocroce	1	0.77	[0.10]	0.42	0.17	0.32	62
Chrysopa	2	0.68 (2.4)	0.12 (0.7)	0.43 (1.9)	0.22 (11)	0.35 (2.4)	84 (2.8)

of 1100 kg m^{-3} has therefore been assumed for use in equation (17). This value is also consistent with the results of Lowndes (1942): he measured the density of some aquatic crustaceans broadly similar in morphology to the insects (Mysidacea, Amphipoda and natantian decapods), and found a mean value of 1100.

The moment of inertia and the location of the centre of mass must be known in order to calculate the response of the body to the forces and moments generated by the wings during flight. Under the assumptions of the graphical technique, the centre of mass must lie on the longitudinal body axis (figure 2*b*). The distance from the centre of the anterior end is given by $\hat{l}$, where

$$\hat{l} = \frac{\Sigma\, a_i\, b_i\, x_i\, \mathrm{d}x_i}{\Sigma\, a_i\, b_i\, \mathrm{d}x_i}. \tag{18}$$

The distance from the forewing base axis to the centre of mass is the radius for the first moment of body mass about that axis, and is therefore denoted by $\hat{l}_1$. It was measured on the lateral-view print after the centre of mass was located, or determined directly in the compound pendulum

technique. The radius of gyration $\hat{l}_2$ for the moment of inertia about the wing base axis is given by

$$\hat{l}_2^2 = I_b/mL^2. \tag{19}$$

To simplify calculations the parallel axis theorem was used to derive

$$\hat{l}_2^2 = \frac{\Sigma\, a_i\, b_i\, x_i^2\, dx_i}{\Sigma\, a_i\, b_i\, dx_i} + \hat{l}_1^2 - \hat{l}^2, \tag{20}$$

where the first term on the right side is the non-dimensional moment of inertia about the y axis. The compound pendulum method may be used to calculate $\hat{l}_2$ directly from equations (2) and (10).

The angle between the longitudinal body axis and the horizontal is defined as the body angle χ in paper III. If the flapping wings generate no mean pitching moments, then the body will assume an angle where the line passing through the wing base and the centre of mass is vertical (figure 2*b*). This free body angle is called x_0, and may be measured directly in the pendulum technique.

4. Discussion

This collection of morphological data is primarily intended for use in the calculations of paper VI, where the biomechanical significance of the parameters will become clear. Because of the small sample sizes, the collection is not suitable for a detailed morphometric analysis of intraspecific variance. Nor should it be amenable to an interspecific allometric analysis, as is commonly done on morphological parameters for flying animals (Osborne 1951; Sotavalta 1952; Greenewalt 1962, 1975; Warham 1977; U. M. Norberg 1981). Such allometric studies require a large range of values for the independent variable before general correlations emerge from the interspecific variations. 'The averaging involved in treating so many different species as a single group will indicate broad trends, but tends to conceal the aerodynamic idiosyncracies of individual species' (Greenewalt 1975). These 'idiosyncracies' are indeed significant: the scatter of points about the general relation on allometric graphs is large, especially when one realizes that it is visually reduced by the logarithmic coordinates. The nature of the morphological parameters derived in this paper is such that they can be divided into two distinct groups: *gross parameters* and *shape parameters*. Over the limited size range of insects in this study, the variation of gross parameters between species is much greater than any systematic variation due to an allometric relation, and no interspecific correlations can be found. The new shape parameters provide quite a surprise, however; intraspecific variances are very low, and extremely strong interspecific allometric relations are found over a small range of parameter values.

4.1. *Gross parameters*

The gross parameters of a flying insect provide a very crude, first-order description of its morphology: a body of given length and mass attached to wings of given length, area and mass. To draw a rough sketch of such an insect we could select the wing length R as a reference length, and draw simple rectangular wings with an aspect ratio appropriate to the wing area. The mean wing thickness, representing the wing mass, could also be sketched on a scale relative to R. The body could be portrayed as a circular cylinder whose length is a given fraction of R, with a diameter corresponding to the body mass.

PHILOSOPHICAL TRANSACTIONS OF THE ROYAL SOCIETY B BIOLOGICAL SCIENCES

Even with this crude sketch the morphological diversity of the insects is readily apparent. The mean diameter of the body is typically 0.16 of the body length, but varies between 0.10 and 0.26. The body length is equal to the wing length on average, ranging from 0.7 to 1.6 times that dimension. The ratio of wing span to mean chord is given by the aspect ratio, which varies from 5.7 to 11.6, with an average value of 8.3. Finally, the mean wing thickness is typically about 0.057 % of the wing length, ranging from 0.015 to 0.106 %. No one insect closely matches this 'average' one, which may not be surprising. The parameters have characteristic values for each species, and show no general interspecific correlations; the absence of an 'average' species is, in fact, consistent with the lack of correlation between parameters. The mean values

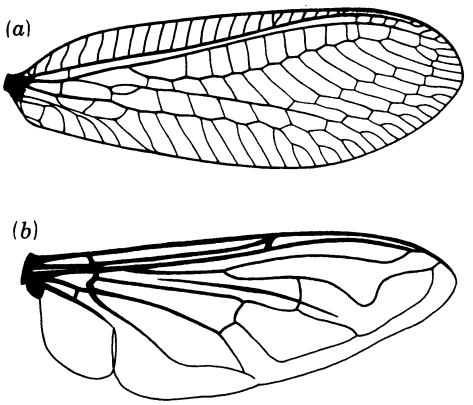

FIGURE 3. Forewing of the green lacewing *Chrysopa carnea* (*a*) and the wing of a drone-fly *Eristalis tenax* (*b*). Although venation is much more extensive, the mass per unit area of the 'primitive' *Chrysopa* wing is less than that of the more 'advanced' *Eristalis* wing.

of the gross morphological parameters must be taken as independent variables for each species, within any broad limits imposed by scaling laws. It would therefore be incautious to use allometric relations to predict morphological parameters for detailed aerodynamic calculations for *specific* animals, as some authors have done. The potential error arising from a single prediction is serious enough, and the errors will compound alarmingly with predictions of several uncorrelated parameters.

The mean wing thickness provides an interesting example of an uncorrelated parameter. Greenewalt (1962) found that the mean thickness increases slightly faster than the wing length over a large size range of birds and insects. This allometric relation is not evident over the small size range of insects considered here, and a predicted value would be quite useless in the face of the observed seven-fold variation in $\hat{h}$. This variation shows no significant correlation with the other gross parameters, but it does seem related to the details of the wing construction. The rich venation of the net-like wings of *Chrysopa* and *Aeschna* is generally considered to be a 'primitive' evolutionary trait. A *Chrysopa* forewing is shown in figure 3 with an *Eristalis* wing for comparison. Although *Eristalis* has much fewer veins, which is characteristic of the 'higher' insects, the veins are more robust than those of *Chrysopa*. The wing membrane of *Eristalis* is thicker as well, resulting in a substantially stiffer wing than in *Chrysopa*. The advanced insects pay a penalty for this wing design, however: the mean wing thickness $\hat{h}$ is typically 0.02 % for *Aeschna* and *Chrysopa*, but is 0.08 % for the advanced insects. Thus the wing mass for a given area is about four times higher for *Eristalis* and the others, and the inertial torque and power

requirement for flapping flight will be increased by the same proportion. The crane-flies have the lowest value of $\hat{h}$ for the advanced insects, and may represent an intermediate stage of wing design. They belong to the dipteran suborder Nematocera, which includes the most primitive of the flies. Venation is fairly complete in the Nematocera and, like $\hat{h}$ for the tipulids, lies between the more advanced and primitive forms.

Before leaving this discussion of gross morphological parameters, the virtual wing mass should be mentioned. This apparent increase in the wing mass is only found during the accelerations of unsteady wing motions; thus it is rarely encountered in conventional aerodynamics, although it is treated in theories of wing flutter. Wing accelerations are certainly large during flapping flight, and significant forces and torques may then arise from the virtual mass. Because it is mechanically analogous to the wing mass, the virtual mass should be considered as another gross parameter. Table 1 shows that it is typically 11% greater than the mass of a cylinder of air with diameter equal to the mean chord and length equal to the wing span: the ratio between the actual value and this reference virtual mass is given by $\hat{v}$.

The virtual mass v has been derived for accelerations of the wings normal to their chords. The strongest accelerations and decelerations in hovering flight occur at either end of the wingbeat, and the chord is nearly perpendicular to the wing motion at these times (paper III). For a first approximation, the inertial effects of the virtual mass can then be calculated based on the assumption that the chord is normal to the wing motion. The ratio of the virtual wing mass to the actual wing mass, v/m_w, then indicates the relative mechanical importance of these two quantities. The virtual mass is easily calculated from equation (14), with a value of 1.23 kg m^{-3} for the density of air at 15 °C and 1 atm (*ca.* 10^5 Pa). The ratio v/m_w is about 0.3 for *Coccinella* and the Diptera, 0.4 for *Manduca* and the Hymenoptera, 0.8 for *Chrysopa* and the forewing of *Aeschna*, and 1.3 for the hindwing of *Aeschna*. The ratios are surprisingly high in general, and demonstrate that the mass of air accelerated by the wings can be fully comparable with the wing mass itself for the light wings of primitive insects like *Chrysopa* and *Aeschna*.

4.2. *Shape parameters*

The mechanics of flight depend not only on the magnitude of gross morphological quantities, but also on their distributions. It will be shown in paper VI that this dependence often hinges on a set of moments about some axis. Thus the mechanical response of the body mass to the cyclic aerodynamic forces is determined by the position of the centre of mass relative to the wing base axis, which is given by the first moment of body mass about that axis, and the moment of inertia of the body, which is equal to the second moment of mass. Similarly, the mechanical effects of wing area, mass and virtual mass depend on their moments about the wing base.

Although these moments have been derived for the biomechanical analysis of hovering flight, they also prove to be very interesting parameters of morphological *shape*. For example, the first three moments of a distribution determine its mean, variance and skewness, which are overall measures of the shape of the distribution. Thus the moments of wing area indicate how the area is distributed along the wing: the shape of the wing planform. Non-dimensional moments normalize the distributions, and their radii provide parameters of shape that can be compared for different animals. These parameters offer a second-order description of an animal's morphology, refining the crude sketch obtained from the gross parameters in § 4.1.

PHILOSOPHICAL TRANSACTIONS OF THE ROYAL SOCIETY B BIOLOGICAL SCIENCES

4.2.1. *Body shape*

It must be remembered that the parameters $\hat{l}$, $\hat{l}_1$ and $\hat{l}_2$ are functions of the mass distribution of the body excluding the leg mass distal to the coxa. When observed under filming conditions, the leg positions vary during some manoeuvres and may shift the centre of mass enough to be beneficial. Because of this, and the assumption of an elliptical body section in the graphical technique, the values of these parameters in table 2 may not be very accurate.

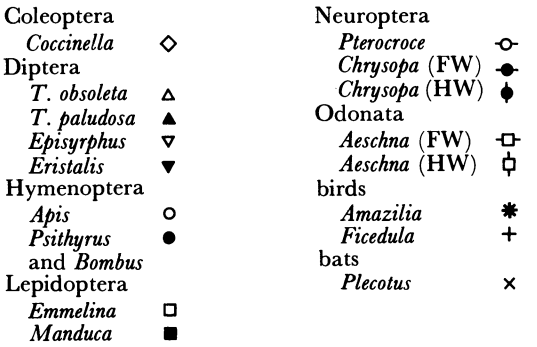

FIGURE 4. Symbols used to identify data from each species, or group, in the graphs of figures 5–9.

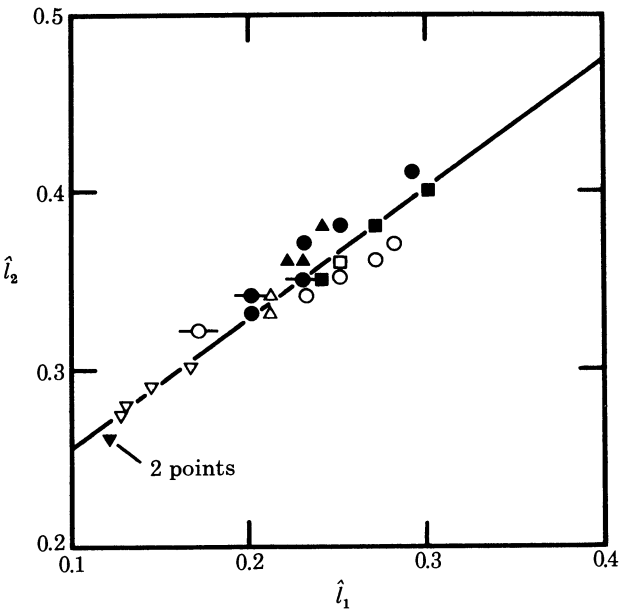

FIGURE 5. Radius of gyration $\hat{l}_2$ for the insect body about the wing base axis is plotted against distance $\hat{l}_1$ from that axis to the centre of mass. The solid line shows the relation obtained by least-squares linear regression.

The location of the centre of mass $\hat{l}$ relative to the body length generally lies at the junction between thorax and abdomen, which agrees with the measurements of Magnan (1934) and the figures of Demoll (1918). The centre of mass is positioned just anterior to this junction in *Eristalis* and *Pterocroce*, and somewhat posterior in *Emmelina*, *Manduca* and the tipulids.

Although correlations between $\hat{l}$ and either $\hat{l}_1$ or $\hat{l}_2$ are very weak, figure 5 shows a correlation between $\hat{l}_1$ and $\hat{l}_2$. The symbols on this graph are identified in figure 4, and they are also used

in figures 6–9. The radius of gyration $\hat{l}_2$ cannot equal zero when the centre of mass lies on the wing base axis ($\hat{l}_1 = 0$) unless the body is a theoretical point mass, and so a simple allometric relation that passes through the origin cannot be justified for the parameters. This would not be the case, however, if the radius of gyration and the position of the centre of mass were measured with respect to the anterior y axis of the body. As the distance between the centre of mass and the y axis decreases to zero, the mass must concentrate on that axis and the radius of gyration would necessarily approach zero, making an allometric relation quite appropriate. These parameters must be measured with respect to the wing base axis in order to investigate the mechanical response of the body, though, and the wing base axis is just an arbitrary point in the body mass distribution. A linear regression has therefore been applied to the data:

$$\hat{l}_2 = 0.182 + 0.736\,\hat{l}_1, \tag{21}$$

which is shown by the solid line in figure 5.

For a given body size (mass and length), the mechanical responses of the body are dependent only on $\hat{l}_1$ and $\hat{l}_2$. By the above result this can be reduced to a dependence on the distance $\hat{l}_1$ from the wing base to the centre of mass, and the mechanical responses may them be changed by a morphological shift in position of the wing bases or the centre of mass. When this distance $\hat{l}_1$ is small, the pitching moments required of the wings to alter the body angle χ are reduced. The moment of inertia I_b, which is proportional to $\hat{l}_2^2$, is also decreased when $\hat{l}_1$ is small and results in greater angular accelerations for given pitching moments. The reduction in I_b produced by small values of $\hat{l}_1$ is certainly significant: when *Eristalis* and *Manduca*, which have the lowest and highest values respectively, are compared, the normalized moment of inertia is decreased by a factor of 2.5. Thus the body is much more responsive in the pitching plane when the wing base is closer to the centre of mass. The response of the body angle is an important determinant of the manoeuvrability of insects because the angle between the body axis and the stroke plane is, for anatomical reasons, roughly constant during flight. As will be discussed in paper III, the stroke plane and body tilt together in a nose-down direction as forward flight speed increases, and tilt nose-up in backward flight. By tilting the stroke plane the insects alter the direction of the mean aerodynamic force produced by the flapping wings, controlling the amount of horizontal thrust and hence their flight speed in a manner analogous to helicopters. Small values of $\hat{l}_1$ enable the body angle and therefore the stroke plane angle to respond quickly to desired changes in speed and direction, increasing manoeuvrability: conversely, larger values of $\hat{l}_1$ should be associated with more sluggish fliers.

The values of $\hat{l}_1$ in table 2 are all similar, except for the notably low values of the hover-fly *Episyrphus*, the drone-fly *Eristalis* and the nemopterid *Pterocroce*. The extreme manoeuvrability of *Episyrphus* and *Eristalis* is readily apparent to the most casual observer in the garden, and they have the lowest values of $\hat{l}_1$. They are also capable of hovering with either an inclined or a horizontal stroke plane (paper III), and this versatility is supported by the reduced pitching moments required to tilt the body angle along with the stroke plane angle. I have never observed a live *Pterocroce* flying, but Weis-Fogh's films reveal it to be a very agile flier within the confinement of a flight cage. Presumably it behaves like other Nemopteridae, flying at dusk and 'dancing' up and down rather like mayflies. The dragonflies are also well known for their manoeuvrability, and Magnan (1934) reports that the centre of mass lies between the forewings and hindwings in *Aeschna parthenope*, a design that should increase the body responsiveness very effectively.

PHILOSOPHICAL TRANSACTIONS OF THE ROYAL SOCIETY B BIOLOGICAL SCIENCES

The free body angle χ_0 is also determined by the relative positions of the wing base axis and the centre of mass, and may represent another morphological adaptation to flight style. This angle is large in the crane-flies, the lacewing *Chrysopa*, and the plume moth *Emmelina*, which are characteristically slow fliers. Since the body angle χ is typically close to this free angle during flight, these insects nearly adopt the correct flight orientation automatically, and pendulum stability of the body will help to maintain this position. The free angle of the hawk moth *Manduca* is also large, and this insect is a very proficient slow flier. *Manduca* is certainly capable of fast flight, however, and would require a large nose-down pitching moment from the wings to maintain the associated body angle. The Hymenoptera, *Episyrphus* and *Eristalis* seem to fly over the entire range of speeds with equal ease, and value of χ_0 near 50° for them may represent a compromise in design.

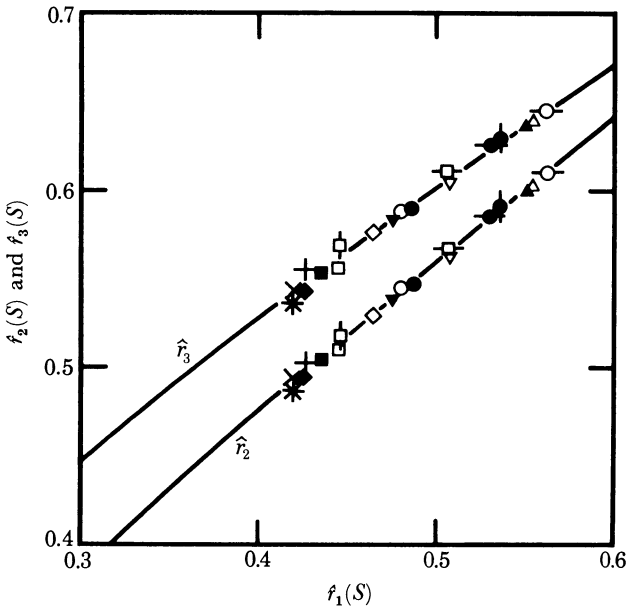

FIGURE 6. Radii of the second and third moments of wing area, $\hat{r}_2(S)$ and $\hat{r}_3(S)$, plotted against position of the centroid $\hat{r}_1(S)$. Values calculated from the approximation of Oehme & Kitzler (1975) for the wing chord distribution of various birds are indicated by a solid diamond. The curves show the allometric relations between these parameters.

4.2.2. *Wing shape*

The most striking feature of the radii of the non-dimensional moments of wing area, mass and virtual mass is the constancy of values for each species in table 1. This is not so apparent for the radii of wing mass, where an average intraspecific coefficient of variation of 4% is largely a result of experimental inaccuracies in the strip-weighing technique. The radii of wing area and virtual mass, however, show an impressive intraspecific variation of only 1% in general: slightly less for the radii of wing area, slightly more for virtual mass. This low variation may be due in part to the global nature of the moment parameters, which makes them fairly insensitive to small local deviations in the distributions. For example, small random deviations in the chord along the length of the wing should have a negligible effect on the moments of area and their radii, but a *systematic* change of the chord distribution must be reflected in the

moments. If the chord near the wing tip is increased, then the position of the centroid of area for that wing, given by $\hat{r}_1(S)$, will shift towards the tip, and all of the moment radii for wing area and virtual mass will increase as well. Thus the differences between species, although small, probably indicate a systematic alteration of the general distributions.

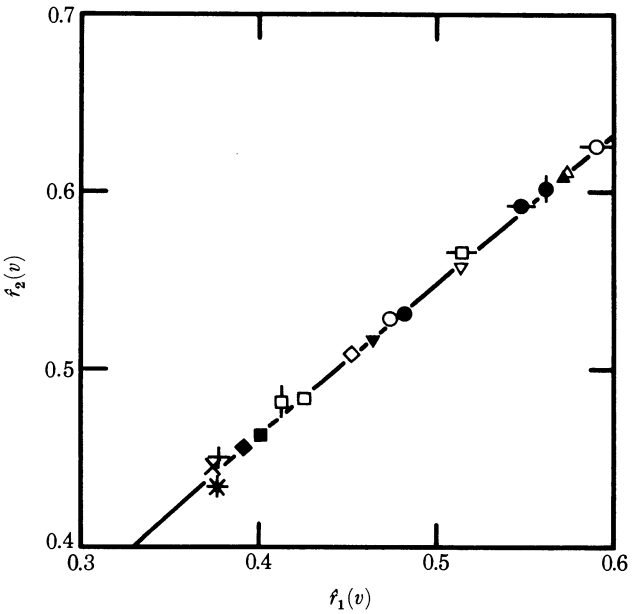

FIGURE 7. Radius of gyration of the virtual wing mass $\hat{r}_2(v)$ is plotted against its centroid $\hat{r}_1(v)$. The value calculated from the approximation of Oehme & Kitzler (1975) for bird wings is indicated by a solid diamond. The allometric relation is shown by the curve.

(*a*) *Laws of shape.* As might be anticipated from the body moment parameters, very strong correlations are found between the radii for wing area, for virtual mass, and those for wing mass. In figure 6 the radii of the second and third moments of wing area, $\hat{r}_2(S)$ and $\hat{r}_3(S)$, are plotted against the position of the centroid of area for a wing, $\hat{r}_1(S)$. Mean values for all groups in table 1 are shown on this graph. The relation between the radius of the second moment of virtual mass $\hat{r}_2(v)$ and its centroid $\hat{r}_1(v)$ is given in figure 7. Similarly, the first and second radii for wing mass are plotted in figure 8. All of the figures show very tight correlations, which is all the more remarkable because the data points represent two birds and a bat as well as the range of insects.

In contrast to the shape parameters of the body, an allometric relation is quite justified for the radii of the wing moment parameters because these moments are taken about the origin of the distributions, the wing base. In the limit as any quantity distributed along the wing becomes concentrated at the wing base, *all* of the moments of that quantity and their respective radii will approach zero. We can therefore assume that two radii, $\hat{r}_m$ and $\hat{r}_n$, can be related by an allometric power function

$$\hat{r}_m = \alpha \hat{r}_n^{\beta}, \tag{22}$$

where the coefficients α and β are found by linear regression of the radii in the logarithmic form of equation (22). The most attractive procedure is to relate all of the higher radii of a

PHILOSOPHICAL TRANSACTIONS OF THE ROYAL SOCIETY B BIOLOGICAL SCIENCES

quantity to $\hat{r}_1$, so that the higher moments can simply be expressed as functions of the position of the centroid. The following allometric expressions are thus obtained:

$$\hat{r}_2(S) = 0.929\ [\hat{r}_1(S)]^{0.732}, \tag{23}$$

$$\hat{r}_3(S) = 0.900\ [\hat{r}_1(S)]^{0.581}, \tag{24}$$

$$\hat{r}_2(v) = 0.929\ [\hat{r}_1(v)]^{0.761}, \tag{25}$$

$$\hat{r}_2(m) = 1.023\ [\hat{r}_1(m)]^{0.817}. \tag{26}$$

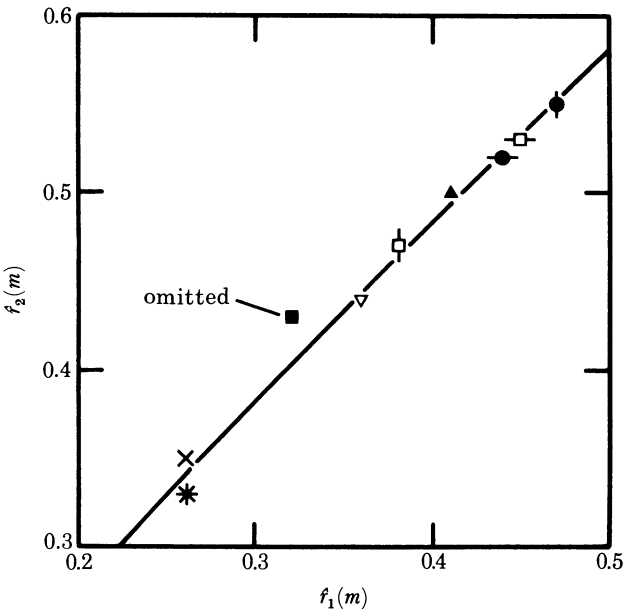

FIGURE 8. Radius of gyration of the wing mass $\hat{r}_2(m)$ is plotted against position of the centre of mass $\hat{r}_1(m)$. As explained in the text, data for *Manduca* were omitted from the allometric regression, which is shown by the curve.

These relations are drawn on figures 6–8. The regression for the wing mass radii does not include the data for *Manduca*, which were measured by the compound pendulum technique instead of strip-weighing. The radius parameters are so exact for a species that differences in experimental technique may well be reflected in their values. Indeed, the *Manduca* data lie outside the 95% confidence limits of the regression for data obtained by strip-weighing.

Allometric relations should also exist between the radii of *different* quantities distributed along the wings. If all of the wing area were concentrated at the wing base, then the wing mass and virtual mass would be as well. This offers the interesting prospect that all of the wing radius parameters could be estimated simply from the centroid of area for the wing. Experimentally, this centroid is easily determined by finding the balance point of the wing planform cut out of an enlarged photograph; the aspect ratio is readily measured as well from the mass of the cut-out and the paper density. The allometric relations between the different radii are

$$\hat{r}_1(v) = 1.47\ [\hat{r}_1(S)]^{1.56}, \tag{27}$$

$$\hat{r}_2(v) = 1.25\ [\hat{r}_1(S)]^{1.19}, \tag{28}$$

$$\hat{r}_1(m) = 1.37\ [\hat{r}_1(S)]^{1.82}, \tag{29}$$

$$\hat{r}_2(m) = 1.32\ [\hat{r}_1(S)]^{1.50}, \tag{30}$$

PHILOSOPHICAL TRANSACTIONS OF THE ROYAL SOCIETY B BIOLOGICAL SCIENCES

where *Manduca* is again excluded from the mass regression. The centroids of mass and virtual mass are plotted against that of wing area in figure 9 to indicate how well the radii of the different quantities correlate. In general, all of the radii for the moments of area and virtual mass can be predicted from $\hat{r}_1(S)$ to an accuracy of about 1–2 %, which is the same magnitude as the mean intraspecific variations. Unfortunately, the allometric relations between the radii of wing mass and $\hat{r}_1(S)$ are not strong enough to be of much predictive value. A better procedure would be to determine the position of the centre of mass $\hat{r}_1(m)$ by balancing the wing on a knife edge, and then to estimate $\hat{r}_2(m)$ from $\hat{r}_1(m)$ by using equation (26).

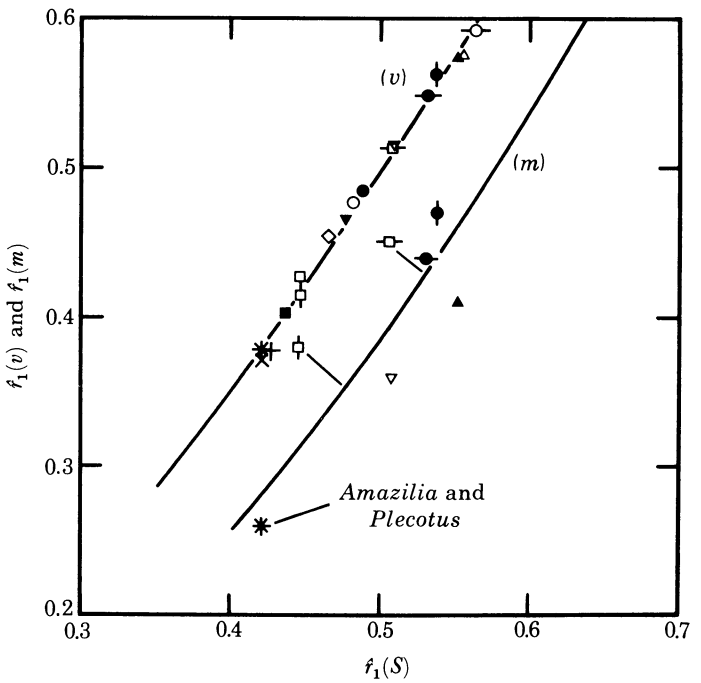

FIGURE 9. Positions of the centroids of virtual mass and mass, $\hat{r}_1(v)$ and $\hat{r}_1(m)$, are plotted against that for wing area $\hat{r}_1(S)$. Allometric relations are indicated by the curve.

It is most improbable that the definite relations between the non-dimensional moments of wing area, mass and virtual mass can be explained by a biological phenomenon common to insects, birds and bats. Aerodynamic and mechanical considerations are much more likely to provide an understanding of the relations, but this approach has been fruitless so far. I am still working on the problem, but we are left at present with precise correlations of experimental data with no basis of understanding. It thus seems appropriate that the allometric relations between the radii should be called *laws of wing shape*: rules that are obeyed even if the reasons for doing so are unknown. These laws are mainly derived from a diverse collection of insects, but two birds and a bat obey the same relations. In fact, many other birds also fit the laws. Oehme & Kitzler (1975) measured the wing chord distribution for 14 bird species differing in size and habits, and found that it could be approximated in general by

$$\hat{c} = \tfrac{6}{5} \quad \text{for} \quad 0 \leqslant \hat{r} \leqslant \tfrac{1}{2}, \quad \hat{c} = \tfrac{24}{5}(\hat{r} - \hat{r}^2) \quad \text{for} \quad \tfrac{1}{2} \leqslant \hat{r} \leqslant 1, \tag{31}$$

where their notation has been made consistent with mine. The radius parameters for wing area and virtual mass are readily calculated from this approximation, and are plotted in figures 6

and 7. An extremely good fit to the other data is evident, so it seems likely that the laws of shape are more generally valid for birds as well as insects.

(*b*) *Weis-Fogh's approximations*. Weis-Fogh (1973) first emphasized the mechanical importance of the moments of wing area, and that they depend on the shape of the wing. Although less general, his 'shape factors' are similar to the radius parameters defined here, which form a consistent set applicable to the moments of other quantities besides area. He approximated nearly all wings by a semi-ellipse for his 'quick estimates', thus assigning a constant value of 0.42 to $\hat{r}_1(S)$. This is the lowest observed value and substantially below the mean of 0.49; his moments of area are underestimated in most cases, therefore, and his aerodynamic calculations must reflect this error. Similarly, his approximation for the mass distribution of the wings sets $\hat{r}_2(m)$ equal to a constant value of 0.41, which is close to the mean of the observed range (0.33–0.55). The moment of inertia is proportional to $\hat{r}_2^2(m)$, though, which equals 0.17 for his approximation and 0.11–0.30 for the observed range. The distributions of quantities along the wing are simply too varied for such rigid approximations to be accurate. This is not meant to detract from Weis-Fogh's pioneering study, however: the approximations were quite suitable for an initial investigation.

(*c*) *Analytical representations of wing shape*. The moment parameters of the wings offer an overall, or global description of their shape. In many applications a more detailed description of shape might be desirable, such as an analytical function for the normalized chord $\hat{c}$ in terms of radial position $\hat{r}$. A general form would have to be *assumed* for the function, incorporating any constants necessary for fitting the general form to the specific data. The success of the assumption is judged by how well the values predicted by the function agree with the observations.

The choice of a suitable function is determined to some extent by the method of fitting constants. A least-squares regression of the function onto the data is an obvious procedure, and almost any analytical function could be fitted by this method; in practice, a simple polynomial or Fourier representation would most likely be selected from the bewildering variety of functions. An alternative scheme is suggested by distribution theory in statistics, however: fitting a distribution function by matching its moments to those of the observed data. This is exactly what is done when data are represented by a normal distribution whose mean and variance are obtained by equating the first two moments of the normal distribution function to those of the data. The method of matching moments seems especially appropriate for the wing shapes, since the moments of data are already required for the biomechanical analysis of flight.

Unlike the normal distribution, which extends from $-\infty$ to $+\infty$, a distribution function suitable for the description of wing shape should be defined over a *limited* interval from 0 to 1. The only standard distribution function for a limited interval is the *Beta distribution*, one of the family of Pearson distributions invented precisely for the representation of experimental data (see Kendall & Stuart 1963). The Beta distribution is defined over the interval of x from 0 to 1, and the distribution function is given by

$$f = x^{p-1}(1-x)^{q-1}/B(p,q), \tag{32}$$

where the Beta function $B(p,q)$ is

$$B(p,q) = \int_0^1 x^{p-1}(1-x)^{q-1}\,\mathrm{d}x. \tag{33}$$

PHILOSOPHICAL TRANSACTIONS OF THE ROYAL SOCIETY B BIOLOGICAL SCIENCES

The distribution is uniquely determined by the two parameters p and q, so the first two moments of the data are sufficient for their estimation. Matching the moments of the Beta distribution to the wing moments, expressed by their radii, gives p and q as

$$p = \hat{r}_1\left(\frac{\hat{r}_1(1-\hat{r}_1)}{\hat{r}_2^2-\hat{r}_1^2}-1\right), \tag{34}$$

$$q = (1-\hat{r}_1)\left[\frac{\hat{r}_1(1-\hat{r}_1)}{\hat{r}_2^2-\hat{r}_1^2}-1\right]. \tag{35}$$

By equating $\hat{c}$ with f and $\hat{r}$ with x in equation (32), and using the radii of wing area in equations (34) and (35), I have compared the Beta distribution with the measured wing chords

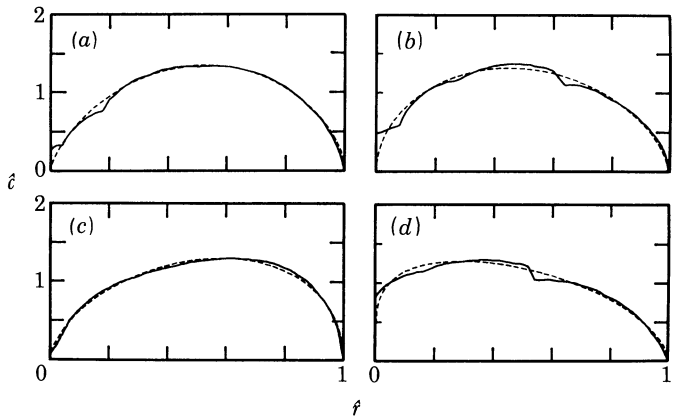

FIGURE 10. Comparison between the non-dimensional chord measured along the wing length (solid line) and the Beta distribution obtained by matching moments (dashed line), for four insects spanning the observed range of $\hat{r}_1(S)$ values: (*a*) *Episyrphus balteatus* (HF08), (*b*) *Bombus hortorum* (BB04), (*c*) *Chrysopa carnea* forewing (LW01), (*d*) *Manduca sexta* (HM02).

for all animals in this study. Figure 10 represents four chord distributions spanning the observed $\hat{r}_1(S)$ values, and the corresponding Beta distributions are shown by dashed lines. The fit ranges form exceptionally good, as for *Episyrphus*, to acceptable, as for *Manduca*. In general, the fit is quite impressive in view of the variety of wing constructions found in the insects, birds and bats; values of $\hat{c}$ predicted by the Beta distribution are typically within 5% of the measured values, and the goodness of fit does not vary systematically with $\hat{r}_1(S)$. Furthermore, the distribution can be reduced to a function of only *one* variable, $\hat{r}_1(S)$, by using the shape law of equation (23) to estimate $\hat{r}_2(S)$, and the resulting distributions are not significantly different from those calculated with the proper values of $\hat{r}_2(S)$. Thus the Beta distribution provides a powerful tool for drawing a close approximation to the entire shape of a wing given only its centroid of area $\hat{r}_1(S)$. Quite unexpectedly, the continuous spectrum of wing shapes can then be described in detail by a *single* parameter of shape.

The Beta distribution is unimodal and falls to zero at either end of the interval, and so it is not a completely suitable description for some wings. Alternatives to it are not obvious, but I have tried a general purpose polynomial distribution function for the wing shape. If the wing chord is represented by

$$\hat{c} = a_0 + a_1\hat{r} + a_2\hat{r}^2 + a_3\hat{r}^3, \tag{36}$$

the radii of the moments of this distribution are then

$$\hat{r}_k^k(S) = \frac{a_0}{k+1} + \frac{a_1}{k+2} + \frac{a_2}{k+3} + \frac{a_3}{k+4}. \tag{37}$$

The coefficients a_0 to a_3 are found by solving the set of simultaneous equations given by $k = 0, 1, 2, 3$ in equation (37). In general, the resulting polynomial distributions fit the chord measurements not quite as well as the Beta distributions, although the fit for more proximal regions of the wing is marginally improved for some insects.

I thank Mr G. G. Runnalls for photographic assistance, and Mr D. M. Unwin for identifying the insects. I am grateful to Dr K. E. Machin for many interesting discussions on the baffling laws of shape, and for a critical reading of the manuscript. Financial support was provided by the Winston Churchill Foundation.

References

Demoll, R. 1918 *Der Flug der Insekten und der Vögel*. Jena: Fischer.
Greenewalt, C. H. 1962 Dimensional relationships for flying animals. *Smithson. misc. Collns.* **144**(2), 1–46.
Greenewalt, C. H. 1975 The flight of birds. *Trans. Am. phil. Soc.* **65**(4), 1–67.
Hoffman, J. D., Lawson, F. R. & Yamamoto, R. 1966 Tobacco hornworms. In *Insect colonization and mass production* (ed. C. N. Smith), pp. 479–486. London: Academic Press.
Jensen, M. & Weis-Fogh, T. 1962 Biology and physics of locust flight. V. Strength and elasticity of locust cuticle. *Phil. Trans. R. Soc. Lond.* B **245**, 137–169.
Kendall, M. G. & Stuart, A. 1963 *The advanced theory of statistics*, vol. 1 (*Distribution theory*). London: Charles Griffin.
Lowndes, A. G. 1942 The displacement method of weighing living aquatic organisms. *J. mar. biol. Ass. U.K.* **25**, 555–574.
Magnan, A. 1922 Les caractéristiques des oiseaux suivant le mode de vol. *Annls Sci. nat.* (ser. 10) **15***b*, 125–334.
Magnan, A. 1934 *La locomotion chez les animaux I. Le vol des insectes*. Paris: Hermann et Cie.
Norberg, R. Å. 1972*a* Flight characteristics of two plume moths, *Alucita pentadactyla* L. and *Orneodes hexadactyla* L. (Microlepidoptera). *Zool. Scr.* **1**, 241–246.
Norberg, R. Å. 1972*b* The pterostigma of insect wings an inertial regulator of wing pitch. *J. comp. Physiol.* **81**, 9–22.
Norberg, U. M. 1975 Hovering flight of the pied flycatcher (*Ficedula hypoleuca*). In *Swimming and flying in Nature* (ed. T. Y. Wu, C. J. Brokaw & C. Brennen), vol. 2, pp. 869–881. New York: Plenum Press.
Norberg, U. M. 1976 Aerodynamics, kinematics and energetics of horizontal flight in the long-eared bat *Plecotus auritus*. *J. exp. Biol.* **65**, 179–212.
Norberg, U. M. 1981 Allometry of bat wings and legs and comparison with bird wings. *Phil. Trans. R. Soc. Lond.* B **292**, 359–398.
Oehme, H. & Kitzler, U. 1975 Untersuchungen zur Flugbiophysik und Flugphysiologie der Vögel. II. Zur Geometrie des Vögelflügels. *Zool. Jb.* (*Physiol.*) **79**, 402–424.
Osborne, M. F. M. 1951 Aerodynamics of flapping flight with application to insects. *J. exp. Biol.* **28**, 221–245.
Sokal, R. R. & Braumann, C. A. 1980 Significance tests for coefficients of variation and variability profiles. *Syst. Zool.* **29**, 50–66.
Sotavalta, O. 1952 The essential factor regulating the wing-stroke frequency of insects in wing mutilation and loading experiments and in experiments at subatmospheric pressure. *Ann. Zool. Soc.* '*Vanamo*' **15**(2), 1–67.
Wainwright, S. A., Biggs, W. D., Currey, J. D. & Gosline, J. M. 1976 *Mechanical design in organisms*. London: Edward Arnold.
Warham, J. 1977 Wing loadings, wing shapes and flight capabilities of Procelariiformes. *N.Z. Jl Zool.* **4**, 73–83.
Weis-Fogh, T. 1972 Energetics of hovering flight in hummingbirds and in Drosophila. *J. exp. Biol.* **56**, 79–104.
Weis-Fogh, T. 1973 Quick estimates of flight fitness in hovering animals, including novel mechanisms for lift production. *J. exp. Biol.* **59**, 169–230.

PHILOSOPHICAL TRANSACTIONS OF THE ROYAL SOCIETY B BIOLOGICAL SCIENCES